11. Milne, G. T. & Weaver, D. T. Dominant negative alleles of RAD52 reveal a DNA repair/recombination complex including Rad51 and Rad52. *Genes Dev.* **7,** 1755–1765 (1993).
12. Mortensen, U. H., Bendixen, C., Sunjevaric, I. & Rothstein, R. DNA strand annealing is promoted by the yeast Rad52 protein. *Proc. Natl Acad. Sci. USA* **93,** 10729–10734 (1996).
13. Kowalczykowski, S. C., Dixon, D. A., Eggleston, A. K., Lauder, S. D. & Rehrauer, W. M. Biochemistry of homologous recombination in *Escherichia coli*. *Microbiol. Rev.* **58,** 401–465 (1994).
14. Wold, M. S. Replication protein A: a heterotrimeric, single-stranded DNA-bindign protein required for eukaryotic DNA metabolism. *Annu. Rev. Biochem.* **66,** 61–92 (1997).
15. Sugiyama, T., Zaitseva, E. M. & Kowalczykowski, S. C. A single-stranded DNA-binding protein is needed for efficient presynaptic complex formation by the *Saccharomyces cerevisiae* Rad51 protein. *J. Biol. Chem.* **272,** 7940–7945 (1997).
16. Sung, P. Yeast Rad55 and Rad57 proteins form a heterodimer that functions with replication protein A to promote DNA strand exchange by Rad51 recombinase. *Genes Dev.* **11,** 1111–1121 (1997).
17. Sung, P. Function of yeast Rad52 protein as mediator between replication protein A and the Rad51 recombinase. *J. Biol. Chem.* **272,** 28194–28197 (1997).
18. Park, M. S., Ludwig, D. L., Stigger, E. & Lee, S. H. Physical interaction between human RAD52 and RPA is required for homologous recombination in mammalian cells. *J. Biol. Chem.* **271,** 18996–19000 (1996).
19. Yonesaki, T. & Minagawa, T. Synergistic action of three recombination gene products of bacteriophage T4, uvsX, uvsY, and gene 32 proteins. *J. Biol. Chem.* **264,** 7814–7820 (1989).
20. Jiang, H., Giedroc, D. & Kodadek, T. The role of protein–protein interactions in the assembly of the presynaptic filament for T4 homologous recombination. *J. Biol. Chem.* **268,** 7904–7911 (1993).
21. Sugawara, N. *et al.* DNA structure-dependent requirements for yeast RAD genes in gene conversion. *Nature* **373,** 84–86 (1995).
22. Rattray, A. J. & Symington, L. S. Use of a chromosomal inverted repeat to demonstrate that the RAD51 and RAD52 genes of *Saccharomyces cerevisiae* have different roles in mitotic recombination. *Genetics* **138,** 587–595 (1994).
23. Kowalczykowski, S. C. & Krupp, R. A. Effects of the *Escherichia coli* SSB protein on the single-stranded DNA-dependent ATPase activity of *Escherichia coli* RecA protein: Evidence that SSB protein facilitates the binding of RecA protein to regions of secondary structure within single-stranded DNA. *J. Mol. Biol.* **193,** 97–113 (1987).

Acknowledgements. We thank T. Ogawa for antibodies against Rad52 and Rad51 proteins, K. Adzuma for advice on the purification of Rad52 protein, E. Zaitsev for strains, and T. Ogawa, A. Shinohara, P. Sung and S. West for communication of unpublished results. This work was supported by grants from the NIH and from the Human Frontier Science Program (to S.C.K.).

Correspondence and requests for materials should be addressed to S.C.K. (e-mail: sckowalczykowski@ucdavis.edu).

Crystal structure of p50/p65 heterodimer of transcription factor NF-κB bound to DNA

Frances E. Chen*, De-Bin Huang†, Yong-Qing Chen† & Gourisankar Ghosh†

*Departments of *Biology, †Chemistry and Biochemistry, University of California, San Diego, 9500 Gilman Drive, La Jolla, California 92093-0359, USA*

The NF-κB p50/p65 heterodimer is the classical member of the Rel family of transcription factors which regulate diverse cellular functions such as immune response, cell growth, and development[1–3]. Other mammalian Rel family members, including the proteins p52, proto-oncoprotein c-Rel, and RelB, all have amino-terminal Rel-homology regions (RHRs)[4–7]. The RHR is responsible for the dimerization, DNA binding and cytosolic localization of these proteins by virtue of complex formation with inhibitor κB proteins[8]. Signal-induced removal of κB inhibitors allows translocation of dimers to the cell nucleus and transcriptional regulation of κB DNA-containing genes[9]. NF-κB specifically recognizes κB DNA elements[1,10,11] with a consensus sequence of 5′-GGGRNYYYCC-3′ (R is an unspecified purine; Y is an unspecified pyrimidine; and N is any nucleotide). Here we report the crystal structure at 2.9 Å resolution of the p50/p65 heterodimer bound to the κB DNA of the intronic enhancer of the immunoglobulin light-chain gene. Our structure reveals a 5-base-pair 5′ subsite for p50, and a 4-base-pair 3′ subsite for p65. This structure indicates why the p50/p65 heterodimer interface is stronger than that of either homodimer. A comparison of this structure with those of other Rel dimers reveals that both subunits adopt variable conformations in a DNA-sequence-dependent manner. Our results explain the different behaviour of the p50/p65 heterodimer with heterologous promoters.

The overall structure of the p50/p65 heterodimer is consistent with that of other Rel family proteins (Fig. 1a)[12,13,31]. Each subunit consists of two immunoglobulin-like domains connected by a 10-amino-acid flexible linker. Dimers form through a β-sheet sandwich of the carboxy-terminal dimerization domains. Unlike most DNA-binding proteins, which use α-helices for base-pair recognition, Rel family dimers use loops from the edges of the N- and C-terminal domains to mediate DNA contacts (Fig. 2a). Secondary structures of the subunits are equivalent, apart from a 32-amino-acid insert in the N-terminal domain of p50 that adds a second α-helix (Fig. 1b) (to simplify description, p50 residues will be written in normal type and p65 residues will be written in italics).

Dimerization in the heterodimer is localized to the C-terminal domains and consists of a hydrophobic core stapled by various polar interactions (Fig. 2b). The backbones of the dimerization domains are highly similar and superimpose with a root-mean-square deviation (r.m.s.d.) of 1.10 Å. The buried surface area upon dimerization is 1,442 Å^2. Of particular interest is the hydrogen bond between homologous residues Asp 254 of p50 and *Asn 200* of p65, which is unique in the heterodimer. In the homodimers, an interaction between homologous residues is energetically unfavourable because this juxtaposes two like charges. Also of interest are nine polar contacts, most of which occur between the backbones of hydrophobic core residues and the side chains of hydrogen-bonding residues. These results are consistent with the observation that the affinity between homodimers of p50 and p65 is weaker than for the heterodimers[14].

The co-crystallized DNA consists of 11 base pairs with a complementary overhanging base on each end (Fig. 1c). The 3′ ten base pairs of the target DNA define the immunoglobulin(Ig) κB element. Analysis of the central 11 base pairs with the program CURVES[15] revealed a 14-degree bend. The bases T_0 and G_{-1} are also twisted out of plane owing to this DNA bending. This DNA bending agrees with biochemical experiments indicating that the p50/p65 heterodimer induces a 17-degree bend in H2-κB DNA[16].

Previous experiments have indicated that the p50 subunit preferentially occupies the 5′ end of an Ig-κB target DNA[2,10,14]. The heterodimer crystal structure not only confirms this orientation, but also demonstrates the exact positioning (Fig. 3a). The observed base-specific contacts support the idea that the Ig-κB site consists of a 5-base-pair 5′-GGGAC-3′ subsite contacted by p50, and a 4-base-pair 5′-TTCC-3′ subsite contacted by p65. Upon binding to DNA, the heterodimer buries 3,754 Å^2 of the total solvent-accessible surface area, of which 58% is derived from interaction with p50. Overall, the DNA contacts mediated by p50 and p65 in the heterodimer structure are similar to those in the homodimer structures[12,13].

Base-specific binding by p50 to the subsite occurs through the residues Arg 54, Arg 56, Tyr 57, Glu 60, His 64 and Lys 241 (Fig. 3b, top). The strict conservation of the first three guanines in the p50 subsite is determined by the hydrogen bonds made by His 64 with the N7 group of G_{-5}, and by Arg 56 and Arg 54 with both the N7 and O6 groups of G_{-4} and G_{-3}. This interaction is strengthened by Glu 60, which hydrogen-bonds with these arginines and makes base-specific contacts to the N4 groups of C_{-5} and C_{-4}. Tyr 57 makes van der Waals contacts with C_{-3} and T_{-2} and is itself strongly

Table 1 Data collection and structure refinement statistics

Data collection

Resolution	Total reflections	Unique data	R_{merge}	I/sigma (last shell)	Completeness (last shell)
2.9 Å	88,449	26,430	0.082	15.8 (3.1)	97.2 (88.6)

Refinement

Resolution (Å)	Reflections ($F_o > 2\sigma$)	Atoms protein/DNA	*R* factor (%)* R_{work}	R_{free}	R.m.s.d. Bonds (Å)	Angles (°)
8.0–2.9	19562	4629/486	21.0	32.1	0.014	1.97

* $R_{work} = \Sigma||F_o| - |F_c||/\Sigma|F_o|$. $R_{free} = \Sigma_T||F_o| - |F_c||/\Sigma_T|F_o|$, where *T* is a test set containing a randomly selected 5% of the observations omitted from the refinement.

restrained by many van der Waals interactions. The bulk of the Tyr 57 side chain results in an absence of purines in the −2, top-strand position in the observed κB sites. The requirement for the nucleotide at position −1 is more relaxed because this base hydrogen-bonds with the flexible Lys 241.

Binding to the 3′ subsite by the p65 subunit occurs through *Arg 33*, *Arg 35*, *Tyr 36*, *Glu 39* and *Arg 187* (Fig. 3b, bottom). The base conservation observed in κB DNA sequences at positions +3 and +4 is a result of the hydrogen bonds formed with *Arg 33* and *Arg 35*. *Glu 39* strengthens this conservation by hydrogen-bonding to the N4 groups of C_{+3} and C_{+4}. Unlike its p50 counterpart Lys 241, the geometry of *Arg 187* is limited by interactions with *Glu 39*, and thus contacts the O4 groups of T_{+2}. Therefore, *Glu 39* defines the base conservation by buttressing these three arginines and forming a highly ordered tetrad. *Tyr 36*, which is constrained by protein contacts in a manner similar to Tyr 57, makes van der Waals contacts to the thymines at positions +1 and +2. Again, a potential steric hindrance with guanines at these sites explains the presence of thymines in most of the known κB sites.

Both p50 and p65 make extensive contacts with the ribose phosphate backbone of DNA: p50 makes 16 and p65 makes 12. Notably, the backbone nitrogens of Gly 65 and Gly 66 make phosphate

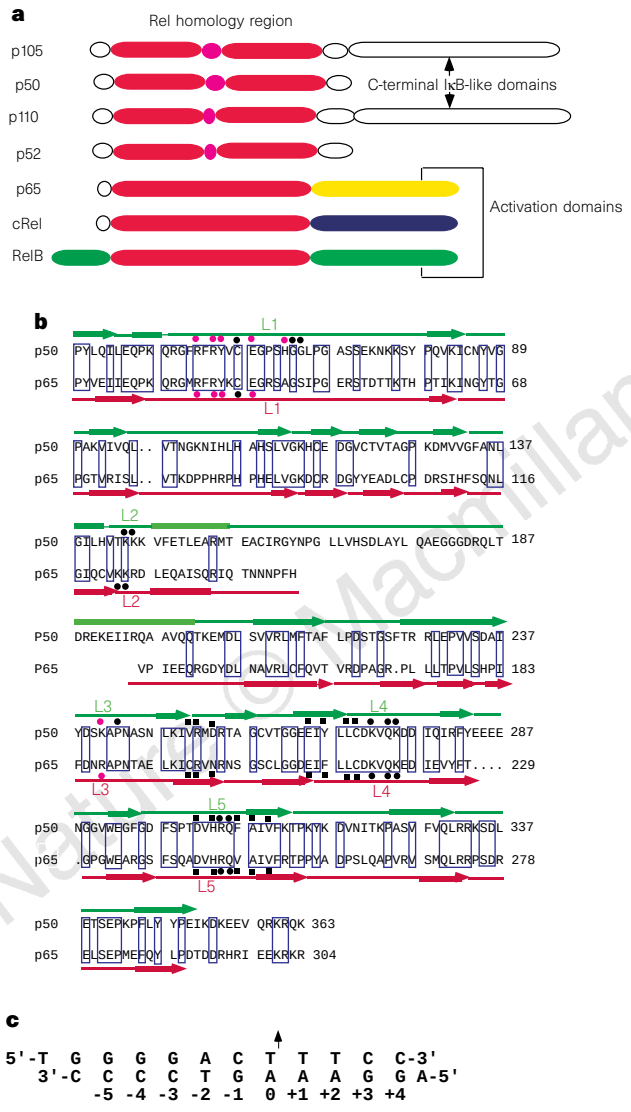

Figure 1 The Rel/NF-κB family of proteins. **a**, Sequence motifs. p50 and p52 are proteolysis products of p105 and p110, respectively, in which the inhibitor (I)κB-like domains are removed. Regions of high homology exist among the family members (RHR) (red ovals). p105(p50) and p110(p52) also contain 32- and 18-amino-acid inserts, respectively, in the RHR (purple ovals). Non-homologous transactivation domains exist in p65, c-Rel, and RelB (different coloured ovals). **b**, Primary sequences and secondary structures of the RHR in mouse p50 (green) and p65 (red) including β-strands (arrow), α-helices (bars), and identical residues (blue boxes). A 32-amino-acid insert exists in p50 after residue 137 in p65. L1–L5 are DNA-contacting loops. Residues that contact DNA (pink circles), contact the DNA backbone (black circles) and contribute to the dimer interface (black squares) are indicated. **c**, The co-crystallized DNA containing the 10-base-pair κB element from the intronic enhancer of the immunoglobulin κ light-chain gene. The two subsites are separated by a pseudodyad T:A base pair (arrow).

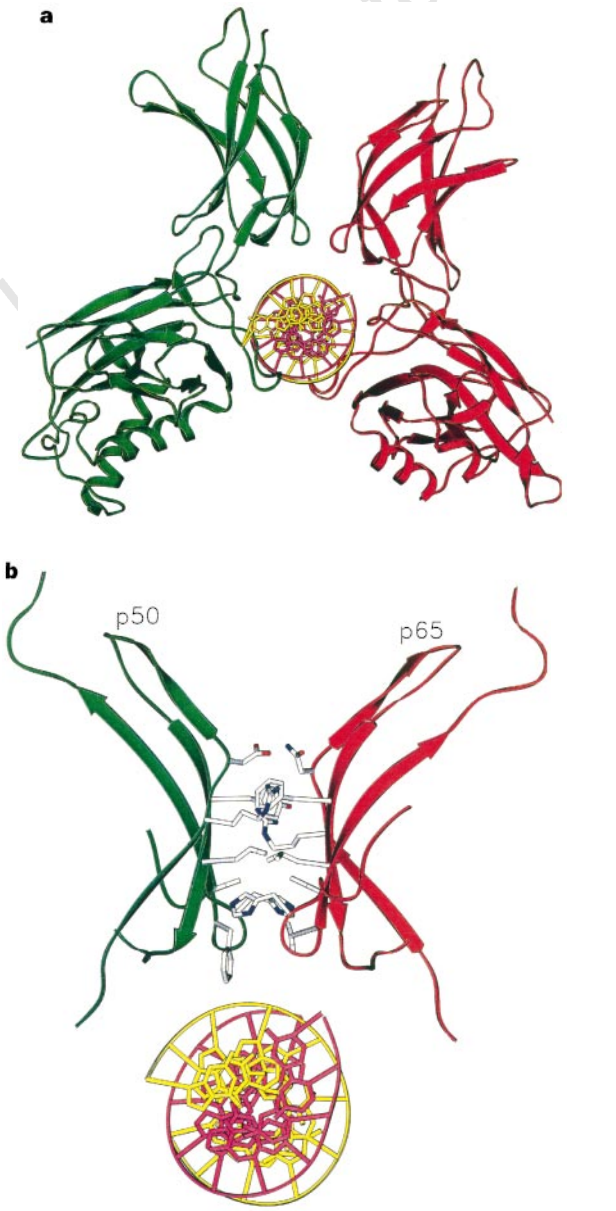

Figure 2 The structure of the heterodimer bound on the Igκ B DNA. **a**, Ribbon drawing of the entire complex viewed down the DNA helical axis. The p50 subunit is in green and the p65 subunit is in red. The top strand of DNA is in pink, and the bottom strand is in yellow. Drawing produced with SETOR[30]. **b**, The hydrophobic core of the dimer interface between p50 (green) and p65 (red) consists of an array of nonpolar hydrocarbons, aromatic rings and uncharged polar residues pointing from the β-sheets in towards the interface. Only the β-strands and seven residues contributing to the interface are displayed. Oxygens (red) and nitrogens (dark blue) are included.

contacts to G_{-6} and G_{-5} and allow His 64 to make proper base-specific contacts. The presence of a side chain at Gly 65 has been found to disrupt DNA binding[17]. Lys 144 and Lys 145 in p50 and the homologous residues in p65, *Lys 122* and *Lys 123*, are the only residues that contact DNA in the minor groove. *Pro 189* also makes van der Waals contacts to the DNA between the deoxyribose moieties of C_{-1} and A_{-2}. Unlike most contacts made by p65, the position of this contact does not exactly mirror the one made in p50 by Pro 243, but is shifted (Fig. 3a). This deviation probably reflects global movements that p65 undergoes to bind this DNA.

The p50/p65 heterodimer has a particularly high DNA affinity compared to most eukaryotic transcription factors: between 10^{-13} to 10^{-10} M (refs 18, 19). This affinity cannot be accounted for by direct DNA readout alone as other transcription factors make similar numbers of contacts. Three other sources might contribute to this high binding affinity. First, interdomain interactions in both subunits might provide a high degree of cooperativity between the two DNA-contacting domains. These interactions result in an interdomain solvent-excluded area of 757 Å^2 for the p65 subunit and 612 Å^2 for the p50 subunit. Second, although the target DNA consists of two subsites, phosphate contacts beyond subsite limits could provide coupling energy in the protein–DNA binding pathway[20]. Finally, the extensive dimer interface could also generate large cooperativity in DNA binding.

Dimerization domain superposition of the p50/DNA half-complex from the heterodimer onto that from the human p50 homodimer reveals that the N-terminal domains require 9 degrees rotation and 2.3 Å translation for superposition[13]. A similar rotation and 1.4 Å translation of the N-terminal domain of p65 is needed when compared to subunit A of the p65/DNA half-complex from the homodimer[31]. The largest component of this rotation occurs around an axis almost parallel to the DNA long axis. Consequently, the base-contacting residues of both subunits move slightly from their optimum positions on DNA.

The p50/p65 heterodimer is the most abundant of the Rel/NF-κB dimers and plays a more elaborate role than other factors in regulating gene expression[2,3]. The p50/p65/Ig-κB DNA complex has served as an archetype for Rel family homo- and heterodimer interaction with DNA targets. Our crystal structure now provides structural information regarding the binding modes of biologically relevant κB DNA targets that do not reflect the observed consensus[10,21,22]. Whereas the 5′ p50 subsite is strictly conserved as 5′-GGGRN-3′, the 3′ p65 subsite is not as well conserved. Conformational adjustments in both subunits are probably necessary for base-specific binding to these κB targets.

Despite architectural differences in the DNAs used for co-crystallization with Rel dimers[12,13], each sequence is bound in a way that preserves the protein–DNA interface chemistry. The subunits' linker regions, in response to the DNA sequence, can adjust the N-terminal domain so that the DNA-contacting residues are aligned properly. Consistent with our observations, the p50/p65 heterodimer has been shown to bend the κB targets H2-κB and IFN-κB, which differ at only three nonconserved bases, by 7 and 17 degrees, respectively[16]. Furthermore, these κB targets do not function in the

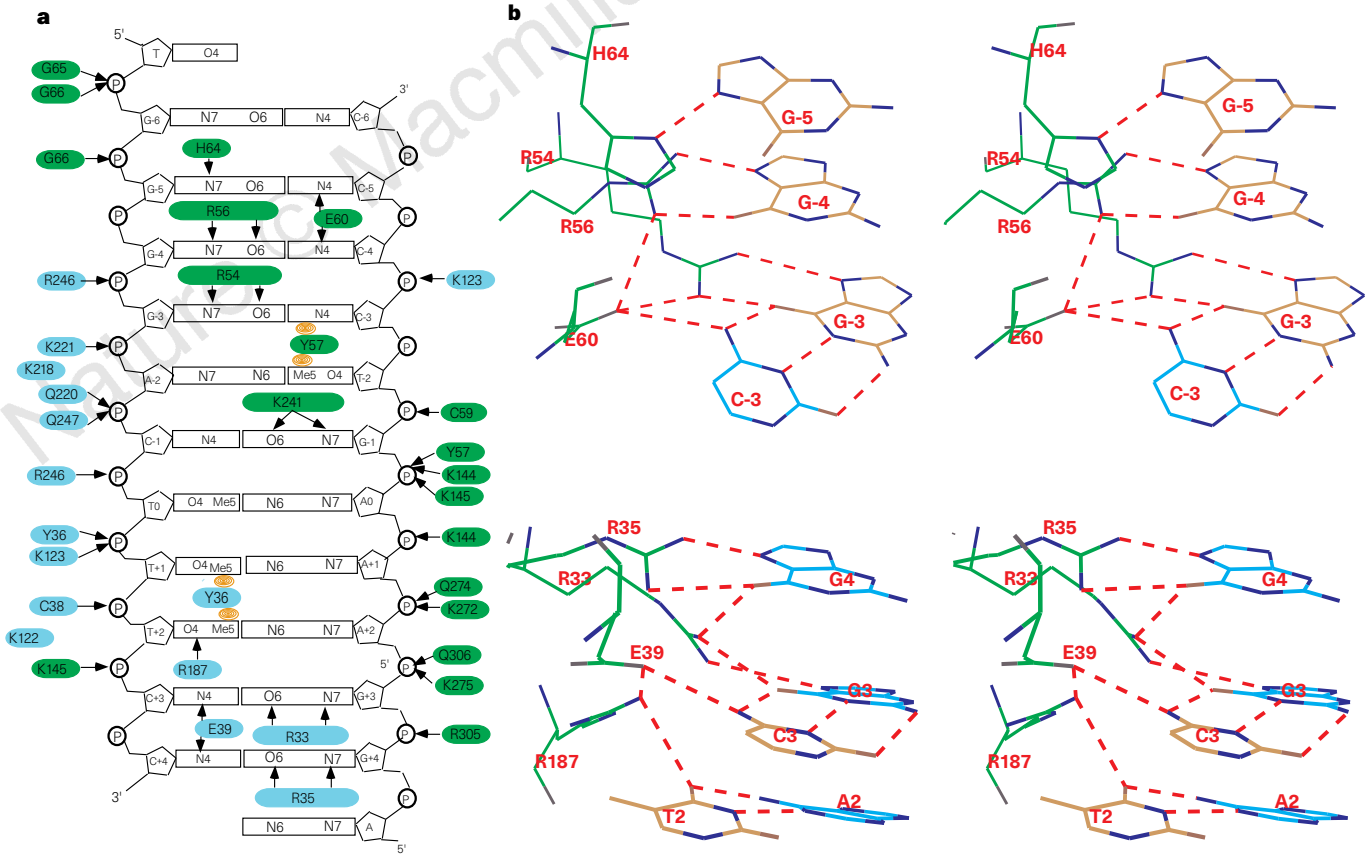

Figure 3 DNA contacts made by the heterodimer. **a**, The DNA contacts made by the p50/p65 NF-κB heterodimer. Blue and green distinguish the p65 and the p50 subunits, respectively. Arrows denote hydrogen bonds; brown ovals indicate van der Waals contacts. The p50 subunit binds to the 5′ five-base-pair subsite; the p65 subunit binds to the 3′ four-base-pair subsite. **b** (top), Stereo pair of the base-specific interactions mediated by Arg 54, Arg 56, Glu 60 and His 64 of the p50 subunit. Hydrogen bonds are drawn as dashed lines between grey oxygens and dark blue nitrogens. p50 residues are green, top strand bases are yellow, while the bottom strand base is in blue. Bottom, Stereo pair of the base-specific interactions mediated by *Arg 34*, *Arg 35*, *Glu 39* and *Arg 187* of the p65 subunit. p65 residues are shown in green.

same manner *in vivo* when placed in heterologous promoters as in their cognate promoters[23]. The combined results of structural, *in vitro* bending, and *in vivo* transcription experiments therefore suggest that the sequence and flexibilities of different DNA targets determine the final conformation of the complexes in a manner sensitive to small differences[18]. □

Methods

Protein purification. Truncated murine p50 (residues 39–364) and p65 (residues 19–291) were overexpressed separately in *E. coli* cells with a T7 promoter driven expression plasmid (Novagen) and purified independently over S-Sepharose (Pharmacia) and Sephadex-75 columns (Pharmacia). The two proteins were combined with a slight molar excess of p65 and unfolded in denaturing buffer (0.5 M NaCl, 7 M urea, 0.5 mM EDTA, 0.1 mM PMSF, 10 mM β-mercaptoethanol, 25 mM Tris-HCl, pH 7.5). The protein was then refolded by dialysis into 20 mM NaCl and 25 mM Tris-HCl, pH 7.5. The renatured heterodimer was purified once again over an S-Sepharose column, concentrated, aliquoted, sorted at −80 °C until needed, and used within 5 h of thawing.

DNA purification. Two 12-base-pair oligonucleotides were synthesized, 5′-TGGGGACTTTCC-3′ and 5′-AGGAAAGTCCCC-3′, by phosphoramidite synthesis. After deblocking, the oligonucleotides were purified over a Q-Sepharose column. Peak fractions were pooled, buffered to 50 mM MES, pH 6.0, desalted, and concentrated to 2 mM in a final buffer of 10 mM Tris-HCl, pH 7.5. Equimolar amounts of both strands were mixed and annealed. The double-stranded oligonucleotide was mixed in 10% molar excess of the p50/p65 heterodimer.

Crystallization and data collection. Crystals grew in nine days at 18 °C ($0.2 \times 0.2 \times 0.4$ mm) from 6-μl hanging drops in a final concentration of 6 mg ml^{-1} complex, 50 mM sodium acetate, pH 5.5, 100 mM $CaCl_2$, 0.125% β-octyl-glucoside, 1 mM spermine, 10 mM dithiothreitol, and 8% polyethylene glycol 3350. Before data collection, crystals were dialysed for two days at 18 °C in 25 μl of 50 mM sodium acetate, pH 5.6, 100 mM $CaCl_2$, 0.125% β-octyl-glucoside, 10 mM dithiothreitol, 1 mM sodium spermine and 15% polyethylene glycol 3350, against 5 ml of a cryosolvent consisting of the same components plus 30% glycerol. Crystals were then mounted in nylon loops and flash-frozen in a liquid nitrogen stream. X-ray diffraction data were collected at 105 K using a Marresearch imaging plate system and X-rays from a large Rigaku rotation anode RU operated at 50 kV and 100 mA. Unit cell dimensions are: $a = b = 106.61$, $c = 206.56$ Å, $\alpha = \beta = \gamma = 90.0°$. The space group is $P4_32_12$. There is one dimer in the asymmetric unit, with a solvent volume fraction of 0.59. Data were indexed and integrated using DENZO and scaled by SCALEPACK[24]. Data collection and reduction statistics are summarized in Table 1.

Structure solution and refinement. The structure of the heterodimer was solved by molecular replacement using X-PLOR[25]. The search model consisted of subunit A from the homodimeric p65/DNA complex and the monomer of human p50/DNA complex. Molecular replacement results showed that $P4_32_12$ is the correct space group. Patterson correlation refinement revealed two solutions: a translation search yielded an R factor 0.46 for solution (1) and 0.48 for solution (2).

The orientation and position of the two solutions were subsequently refined by rigid-body refinement using 10.0 to 3.5 Å data. Refinement was performed first on the whole molecule, then the two subunits, and finally by allowing each domain to move independently. This resulted in an R factor of 0.39 for solution (1) and 0.47 for solution (2). Hence, solution (1) was chosen as a starting model. Successive cycles of positional refinement and simulated annealing in X-PLOR combined with model rebuilding progressively improved the structure. Manual adjustments were made based on $|2F_o - F_c|$ difference maps on SGI graphics workstations using programs TOM[26] and O (ref. 27). The parameter set of Engh and Huber[28] was applied for the structure refinements. Inclusion of individual isotropic temperature factors in the refinement resulted in a final R factor of 0.21 and an R_{free} of 0.32. Ramachandran plots generated with PROCHECK[29] showed that 96% non-glycine residues were in the most favoured regions (70%) and additional allowed regions (26%) in both subunits. Of the 1% residues with ϕ and ψ angles in disallowed regions, all are located in the loop areas. The final refinement statistics and stereochemical parameters are presented in Table 1.

Received 15 July; accepted 30 September 1997.

1. Sen, R. & Baltimore, D. Inducibility of κ immunoglobulin enhancer-binding protein NF-κB by a post-translational mechanism. *Cell* **47,** 921–928 (1986).
2. Baldwin, A. S. Jr The NF-κB and I κB proteins: new discoveries and insights. *Annu. Rev. Immunol.* **14,** 649–683 (1996).
3. Siebenlist, U., Franzoso, G. & Brown, K. Structure, regulation and function of NF-κB. *Annu. Rev. Cell. Biol.* **10,** 405–455 (1994).
4. Ghosh, S. *et al*. Cloning of the p50 DNA binding subunit of NF-κB: homology to rel and dorsal. *Cell* **62,** 1019–1029 (1990).
5. Kieran, M. *et al*. The DNA binding subunit of NF-κB is identical to factor KBF1 and homologous to the *rel* oncogene product. *Cell* **62,** 1007–1018 (1990).
6. Nolan, G. P., Ghosh, S., Liou, H. C., Tempst, P. & Baltimore, D. DNA binding and I κB inhibition of the cloned p65 subunit of NF-κB, a rel-related polypeptide. *Cell* **64,** 961–969 (1991).
7. Ruben, S. M. *et al*. Isolation of a rel-related human cDNA that potentially encodes the 65-kD subunit of NF-κB. *Science* **251,** 1490–1493 (1991).
8. Baeuerle, P. A. & Baltimore, D. I. κB: a specific inhibitor of the NF-κB transcription factor. *Science* **242,** 540–546 (1988).
9. Chen, Z. *et al*. Signal-induced site-specific phosphorylation targets I κB alpha to the ubiquitin-proteasome pathway. *Genes Dev.* **9,** 1586–1597 (1995).
10. Zabel, U., Schreck, R. & Baeuerle, P. A. DNA binding of purified transcription factor NF-κB. Affinity, specificity, Zn^{2+} dependence, and differential half-site recognition. *J. Biol. Chem.* **266,** 252–260 (1991).
11. Lenardo, M. J. & Baltimore, D. NF-κB: a pleiotropic mediator of inducible and tissue-specific gene control. *Cell* **58,** 227–229 (1989).
12. Ghosh, G., van Duyne, G., Ghosh, S. & Sigler, P. B. Structure of NF-κB p50 homodimer bound to a κB site. *Nature* **373,** 303–310 (1995).
13. Müller, C. W., Rey, F. A., Sodeoka, M., Verdine, G. L. & Harrison, S. C. Structure of the NF-κB p50 homodimer bound to DNA. *Nature* **373,** 311–317 (1995).
14. Urban, M. B., Schreck, R. & Baeuerle, P. A. NF-κB contacts DNA by a heterodimer of the p50 and p65 subunit. *EMBO J.* **10,** 1817–1825 (1991).
15. Lavery, R. & Sklenar, H. The definition of generalized helocoidal parameters and of axis curvature for irregular nucleic acids. *J. Biomol. Struct. Dyn.* **6,** 63–91 (1988).
16. Falvo, J. V., Thanos, D. & Maniatis, T. Reversal of intrinsic DNA bends in the IFN-β gene enhancer by transcription factors and the architectural protein HMB I(Y). *Cell* **83,** 1101–1111 (1995).
17. Toledano, M. B., Ghosh, D., Trinh, F. & Leonard, W. J. N-terminal DNA-binding domains contribute to differential DNA-binding specificities of NF-κB p50 and p65. *Mol. Cell. Biol.* **13,** 852–860 (1993).
18. Thanos, D. & Maniatis, T. The high mobility group protein HMB I(Y) is required for NF-κB-dependent virus induction of the human IFN-β gene. *Cell* **71,** 777–789 (1992).
19. Urban, M. B. & Baeuerle, P. A. The 65-kD subunit of NF-κB is a receptor for I κB and a modulator of DNA-binding specificity. *Genes Dev.* **4,** 1975–1984 (1990).
20. Klemm, J. D., Rould, M. A., Aurora, R., Herr, W. & Pabo, C. O. Crystal structure of the Oct-1 POU domain bound to an octamer site: DNA recognition with tethered DNA-binding modules. *Cell* **77,** 21–32 (1994).
21. Whitley, M. Z., Thanos, D., Read, M. A., Maniatis, T. & Collins, T. A striking similarity in the organization of the E-selectin and β-interferon gene promoters. *Mol. Cell. Biol.* **14,** 6464–6475 (1994).
22. Hansen, S. K., Guerrini, L. & Blasi, F. Differential DNA sequence specificity and regulation of HIV-1 enhancer activity by cRel-RelA transcription factor. *J. Biol. Chem.* **269,** 22230–22237 (1944).
23. Cross, S. L., Halden, N. F., Lenardo, M. J. & Leonard, W. J. Functionally distinct NF-κB binding sites in the immunoglobulin κ and IL-2 receptor α chain genes. *Science* **244,** 466–469 (1989).
24. Otwinowski, Z. in *Proceedings of the CCP4 Study Weekend: Data Collection and Processing* (eds Sawyer, L., Isaacs, N. & Bayley, S.) 56–62 (SERC Daresbury Laboratory, Warrington, UK, 1993).
25. Brünger, A. T. *X-PLOR Version 3.1: A System for X-ray Crystallography and NMR* 1–382 (Yale University Press, New Haven, 1992).
26. Cambillau, C. & Horjales, E. TOM: a FRODO subpackage for protein ligand fitting with interactive energy minimization. *J. Mol. Graph.* **5,** 174–177 (1987).
27. Jones, T. A., Zou, Y., Cowan, S. W. & Kjeldgaard. Improved methods for binding protein models in electron density maps and the location of errors in these models. *Acta Crystallogr. A* **47,** 110–119 (1991).
28. Engh, R. A. & Huber, R. Accurate bond angle parameters for X-ray protein structure refinement. *Acta Crystallogr. A* **47,** 392–400 (1991).
29. Laskowski, R. A., MacArthur, M. W., Moss, D. S. & Thornton, J. M. PROCHECK: a program to check the stereochemical quality of protein structure coordinates. *J. Appl. Crystallogr. A* **42,** 140–149 (1993).
30. Evans, S. V. SETOR: hardware-lighted three-dimensional solid model representations of macromolecules. *J. Mol. Graph.* **11,** 134–138 (1993).
31. Chen, Y. Q., Ghosh, S. & Ghosh, G. A novel DNA recognition mode by NF-κB p65 homodimer. *Nature Struct. Biol.* (in the press).

Acknowledgements. We thank S. Kempiak for help with protein purification and T. Huxford and S. Malek for critically reading the manuscript. This work was supported by fellowships from the NSF and the Lucille P. Markey Charitable Trust to F.C. Y.-Q.C. is a fellow of the Irvington Institute of Medical Research. G.G. is a recipient of a young investigator award from the university wide AIDS research program. This work is supported by a NIH research grant to G.G.

Correspondence and requests for materials should be addressed to G.G. (e-mail: gghosh@chem.ucsd.edu). Coordinates have been deposited in Brookhaven Protein Data Bank under accession code 1VKX.